

Experimental investigation of high velocity oblique impact and residual tensile strength of carbon/epoxy laminates

Ashwin R Kristnama^{1*}, Xiaodong Xu¹, David Nowell^{2,3}, Michael R Wisnom¹, Stephen R Hallett¹

¹Bristol Composites Institute (ACCIS), University of Bristol, University Walk, Bristol BS8 1TR, UK.

²Imperial College London, London, SW7 2AZ

³University of Oxford, Oxford, OX1 3PJ

Abstract

Composite components are required to be resilient against Foreign Object Damage (FOD) induced by localised high velocity impact events. Here an experimental investigation into high velocity oblique impacts and residual tensile strength of thin quasi-isotropic carbon/epoxy laminates is reported. Oblique (45°) impacts between 100 m/s and 350 m/s were carried out using 3mm steel cubes on the edge and the centre of the laminates, mounted as a cantilever beam. Impact induced damage was characterised using X-ray Computed Tomography (CT) and the residual strength of impacted laminates was determined through quasi-static tensile tests. The residual strength shows a strong dependence on the impact damage size, characterised in terms of fibre fracture width and delamination area. Machined notches were then investigated and compared to impacted laminates in terms of residual strength.

Keywords: A. Laminate, B. Impact behaviour, B. Strength, C. Notch

1. Introduction

Aircraft structures and components are subject to harsh operating environments which make them vulnerable to damage. The effect of foreign object

*Corresponding author: ak0208@bristol.ac.uk (AR Kristnama)

damage (FOD) on composite structures represents a high level of concern, with various forms of damage such as matrix cracks, delamination, fibre/matrix debonding and fibre fracture [1]. The combination of these factors may result in premature or unpredicted failures. For these reasons, FOD has been identified as a major challenge both in terms of maintenance costs and potential safety issues. To improve FOD resistance at an early design stage, it is important to understand the mechanisms behind high velocity impact damage in composite materials.

A substantial amount of work has been published over the years to investigate impact damage in composites, referring to low, medium and high velocity impacts, which are synonymous with low and high strain-rates [2-12]. *Cantwell and Morton* [3] worked on low and high velocity responses of Carbon Fibre Reinforced Polymer (CFRP) laminates with different stacking configurations and varying thicknesses (0.5 – 4.0 mm). Matrix cracking and tensile/flexure failure in the reinforcing fibres were the main damage mechanisms at low velocities, while at higher velocities, complete perforation of the laminates was observed, with significantly greater delamination. While some authors have focussed on ballistic response of complex CFRP structures [9, 13], others have studied single specimens of relatively thin laminates [3, 4, 6-8, 10, 12], where the hardness and strength of the projectile are very much greater than those of the target. For example, *Lopez-Puente et al.* [4] investigated normal and oblique (45°) responses of a 2.2 mm thick woven CFRP laminate impacted with a 1.73 g spherical steel projectile of 7.5 mm diameter, for impact velocities between 70 and 531 m/s. Below the impact energy required for initiating penetration, the composite is assumed to absorb all the kinetic energy of the projectile mainly in the form of damage, which involves delamination. Above the ballistic limit, a cylindrical penetration path due to

the shape of the projectile is more pronounced and the damage extension decreases with increasing velocity. The authors also concluded that the damage extent above the ballistic limit is greater as impact obliquity is increased. However, their work did not extend to look at residual strength after impact. In a more recent study conducted by *Cui et al.* [14] to predict impact damage in composites using Puck and LaRC failure criteria, impact tests were carried out at 90° and 45° on 5 mm thick IM7/8552 composite plates for a velocity range of 21 – 157 m/s. A 20 mm diameter steel ball of mass 32.7 g was employed. For low and medium impact velocities, delamination was observed to be the dominant failure mode. As the velocity is increased, more fibre failure and splitting were noticed.

For composite structures, ballistic impact causes damage which generally extends to a significantly larger region than the visible damage area. The residual strength of composite structures with a combination of visible penetration damage and internal damage is not well understood. Very limited research has been conducted in measuring the residual strengths of composite structures subject to ballistic impacts [15, 16]. *Dorey and Sidey* [15] used a 6 mm diameter steel projectile fired from an airgun with impact speed up to 300 m/s to investigate ballistic response of carbon/epoxy composite laminates of thickness 3 mm with quasi-isotropic layup. Tensile tests were conducted post impact to determine the residual strength. Specimens impacted at the ballistic limit speed of 60 – 80 m/s showed maximum damage and lowest residual strength. Above the ballistic limit, relatively clean holes were punched and the residual strength is increased. Generally, it is mandatory to carry out impact tests, and then tension or compression tests to determine the residual strength of an impacted component. During the preliminary design phase, it is

interesting to investigate the equivalence in strength reduction between impacted and notched laminates to see if this might offer a simpler way to assess the effect of impact damage. Several studies have compared impacted laminates to laminates with a circular hole [17-19] or an elliptical hole [20], but only for Compression After Impact (CAI) tests. This study takes a new approach in comparing machined notches as a potential equivalent for tension after impact tests. Components found in aircraft engines may undergo compressive, tensile and cyclic loads. While CAI has been the standardised strength measurement, tension after impact is also important for structural components subjected to high tensile forces, where the strength reduction is expected to be strongly dependent on the extent of fibre failure.

Various experiments on high velocity impact with larger and heavier spherical projectiles have been reported [4,10,12,14,21]. A few articles studied the influence of obliquity in high velocity impacts for woven [4,10,12] and unidirectional carbon/epoxy laminates [21]. For carbon/epoxy laminates, 45° impacts were observed to induce a larger extent of damage than 90° impacts at high velocities. In addition, there is no research conducted to investigate the equivalence in residual tensile strength between high velocity impacted laminates and laminates with machined notches. To this end, this paper focusses on a combination of high velocity oblique (45°) impacts at two different positions on quasi-isotropic carbon/epoxy laminates and the effect of impact damage on the residual tensile strength. X-Ray Computed Tomography (CT) scanning is carried out to characterise the impact damage. Furthermore, machined notches of equivalent sizes are investigated for their residual strengths.

2. Materials and procedure

The material used was Hexcel HexPly® IM7/8552 carbon-epoxy pre-preg with a ply thickness of 0.125 mm. The laminates have a quasi-isotropic stacking sequence $[45/90/-45/0]_{2s}$ and a nominal fibre volume fraction of about 60% according to the manufacturer's specifications. The prepared laminates were cut into rectangular specimens 250 mm long and 40 mm wide. The nominal overall thickness is 2 mm, which is very close to the actual specimen thickness.

High velocity impacts were conducted employing the gas gun facility shown in Figure 1 [22]. The apparatus consists of a compressed gas reservoir, a breech, a pair of clamps, a barrel, a sabot arrester and a target support. The gun barrel is 1.3 m long with a bore diameter of 12.5 mm. A cylindrical sabot is used to support a 3 mm steel cube projectile, weighing 0.22 g, during the acceleration along the barrel. While previous studies have conducted high velocity impacts with larger and heavier spherical projectiles, a cube projectile was chosen for this study. This is because a cube is more representative of small, hard and sharp-edged fragments which are ingested in aircraft engines. With the projectile fitted inside the breech and clamped in position, the pressure is slowly raised to the desired value, and clamps are then released causing the sabot to accelerate along the barrel. The sabot is stopped by the sabot arrester, and the projectile moves ahead by inertia. The projectile strikes the target, which is supported at its base as a cantilever. A mechanical fixture, which holds the target, is allowed to rotate about the longitudinal specimen axis (Y axis) and translate perpendicular to the gun axis (X axis). It can also be adjusted for height (Y axis). This facilitates positioning of the target in front of the barrel at the desired impact angle

and position along the target edge. The target is clamped over a length of 40 mm from one end onto the mechanical fixture, which is rigidly fixed during the tests. Two optical sensors placed 50 mm apart along the barrel record the time as the sabot passes these two points. The velocity of the projectile was varied from 100 m/s to 350 m/s, at intervals of 50 m/s. Previous work has shown negligible rotation of the sabot and projectile in the barrel of the gun [23], however it was not possible to control the rotation of the cube once it leaves the sabot. For edge impacts, the projectile was aimed to strike the target at a point which is 1.5 mm from the edge, to ensure contact between the projectile and the target. For centre impacts, the projectile was aimed to hit the target exactly at the centre point of the laminate's width. The impact points are shown in Figure 2. Due to the projectile's oblique trajectory, it is motivating to investigate the extent of impact damage close to the edge and far away from the edge of the target, which is why the current two representative impact positions were chosen. A total of 65 specimens were manufactured and tested, where 5 specimens were allocated for each impact configuration and the remaining 5 specimens were used for testing non-impacted laminates. Table 1 provides details on the recorded incident impact velocities for all configurations, where the consistency can be confirmed by the low C.V values (0.5 – 5.4 %).

Machined notches were made at the edge and at the centre of the laminates, as illustrated in Figure 3. The laminates for each notch length were cut on a Computer Numerical Control (CNC) milling machine. Using a 1 mm diameter end mill, machined notches of lengths based on the dimensions in Table 2 were made. To determine the residual strength of impacted and notched laminates, tensile tests were carried out using a 100 kN Instron hydraulic-driven test machine according to the ASTM D3039

standard [24]. In this work, no end tabs were used for all laminates tested. The specimens were loaded in the 0° fibre orientation (aligned with the y-axis in Figure 3) and were tested under displacement control, with a loading rate of 1 mm/min. The internal damage and fibre failure were inspected via CT scanning of impacted laminates. A single specimen from each impact configuration was examined. The samples were soaked in a bath of zinc iodide penetrant for 24 hours. A Nikon XTH225ST CT scanner, with a 3 µm focal spot size, was employed. The scanning voltage was 55 kV and current 145 µA, with an exposure time of 700 ms for each radiograph.

3. Results

In this section, an analysis of the impact damage and the residual tensile strength of the impacted laminates is presented. While the extent of damaged area as a function of the absorbed energy has been commonly used to quantify impact damage, the present study focussed on characterising impact damage in terms of fibre fracture and delamination area. These two parameters are considered because the residual tensile strength is dependent on the impact damage size, and the effect of fibre fracture and delamination area on the residual strength is examined. In addition, the residual strength of machined notches is investigated and compared against residual strength of impacted laminates.

3.1. Damage characterisation

As it is the 0° plies which carry most of the post-impact tensile load, the distance over which the fibres are broken was measured in all the 0° plies. Figure 4 provides illustrations of CT scans for edge impacted laminates at 200 m/s and 350 m/s, while Figure 5 shows CT scans for centre impacted laminates at 200 m/s and 350 m/s.

The widths, w , of broken 0° fibres in both edge and centre impacted laminates were measured and are shown in Figures 4 and 5. CT scan images were uploaded to the ImageJ® software. The image width is 175 pixels, corresponding to 40 mm. A horizontal line was drawn corresponding to w and its length, in terms of its number of pixels, was obtained. The latter was then translated to obtain the equivalent value of w in mm. The definition of w was made by considering the light patches, which represent the extent of fibre fracture and can be easily distinguished from the surrounding dark patches. The dark areas around the light patches represent remaining fibres around the impact point, and were not considered when measuring w . The fibre failure due to impact, termed as fibre fracture width, is determined as the widths of broken fibres in the 0° plies averaged over the number of 0° plies broken. Table 2 provides details on the number of broken 0° plies and the fibre fracture widths for both edge and centre impacted laminates. The fibre fracture in the 0° plies was considered to calculate the fibre fracture width, but the extent of fibre fracture in other plies could become relevant in the cases where the applied post-impact load is not aligned with the 0° plies. As such, the extent of fibre failure in all plies was inspected and found to differ from the fibre fracture widths in Table 2, by an average difference of 3.9%. Since the laminates are loaded along the 0° orientation in the post-impact tests conducted here, the fibre fracture width based on the 0° plies only was considered sufficient. As the impact velocity is increased to 350 m/s, the extent of fibre fracture is larger than the size of the projectile because of the oblique trajectory of the projectile during penetration. In addition, the local bending, the multiple ply orientations and development of different damage modes around the impact site cause a larger extent of fibre failure than just the area under the impactor.

Through the thickness, there is a double 0° ply block at the central symmetry plane, but outboard only single 0° plies. For an edge impacted laminate at 100 m/s, only the top outboard 0° ply showed fibre breakage. When the impact velocity was increased to 200 m/s, all the 0° plies were broken. Complete perforation of edge impacted laminates was observed at 300 m/s. CT scan images for centre impacts at 100 and 150 m/s did not reveal fibre failure in any 0° plies, and only fibres broken in the top 45°, 90° and -45° plies were observed for impact at 150 m/s. For centre impacts at velocities between 200 m/s and 300 m/s, three out of four 0° plies were observed to have fibres broken. At 350 m/s, the centre impacted laminate exhibited broken fibres in all four 0° plies. Careful examination of all plies revealed laminate perforation at 350 m/s in the centre impacted specimen.

Another characteristic feature of impact damage is delamination, which is represented by the slightly darker patches in Figure 6, where typical -45°/0° interfaces for edge impacts at 200 m/s and 350 m/s are illustrated. All the interfaces within the laminates were inspected from CT scans. The area enclosed within the region marked in white, shown in Figure 6, represents the delaminated area for one interface. The white patterns in Figure 6 were drawn using a freehand option available in the ImageJ® software and possible measuring errors could be linked to either adding or subtracting material while sketching. The image width is 175 pixels, with one pixel corresponding to 228 µm. As the height of the scanned laminates vary for different impact configurations, the image height varies between 265 – 340 pixels. The area within the region showing delamination was then determined in terms of its number of pixels and translated to a value equivalent to the area, in mm². The extent of the delaminated

area for each interface was measured and the delamination area was obtained by averaging over the 15 interfaces within the laminate.

The variation in delamination area with impact velocity for edge and centre impacts is represented in Figure 7. For both impact cases, smaller damaged areas were observed in interfaces close to the impact point. Away from the impact point, the maximum damaged areas increased in size, as confirmed by the tops of the error bars in Figure 7. For edge impacts, the delamination area increases with increasing impact velocity until it reaches a maximum value, after which it decreases in size as impact velocity is increased. For centre impacts, the delamination area also increases with increasing impact velocity, but with a slower rate of increase for velocity beyond 300 m/s. At lower impact velocities, an edge impacted laminate shows larger delamination area than a centre impacted laminate. Whereas at a maximum impact velocity of 350 m/s, centre impacted specimen was observed to have a larger delamination area than edge impacted specimen, which shows the effect of impact position on delamination area. The larger delamination area in the centre impacted specimens can be associated with the greater constraint at the impact point where, due to symmetry of the central impact geometry there is no rotation of the laminate, leading to higher local interlaminar shear stresses whereas for edge impacts, the edge is free to rotate upon impact.

3.2. Residual tensile strength

Typical load-crosshead displacement responses of the unnotched, edge and centre impacted laminates at impact velocity of 350 m/s are shown in Figure 8. Edge and centre impacted laminates show an almost linear response up to failure, where a

fibre pull-out mechanism can be observed near the impact damage front at the failure load. The unnotched laminate failed near the grips and its non-linearity is possibly due to slippage at the grips during the test. From these load-crosshead displacement responses, the highest load level is taken as the failure load, from which the tensile strength is calculated using Eq. 1.

$$\sigma = \frac{P_{failure}}{A} \quad (1)$$

where, σ is the tensile failure stress, $P_{failure}$ is the average peak load recorded at failure and A is the full cross-sectional area of the undamaged laminate, obtained from the measured widths and nominal thicknesses of individual specimens. Both gross-sectional and net cross-sectional area have been used in the literature to represent the notched strength. In this study, gross-sectional area was chosen to maintain consistency with previous works [25,26]. The residual strength based on net cross-sectional area can easily be calculated by the readers using the fibre fracture width and sample width in the paper.

The tensile strength for unnotched laminates is 909 MPa (C.V. 2.2%), considered reasonable as it is lower by only 5.7% than the unnotched tensile test results for a quasi-isotropic laminate with similar lay-up and volume of 0° plies [27]. Table 3 summarises the residual tensile strength for the two impact cases at all impact velocities. No significant reduction in strength was observed for centre impacted laminate at 100 m/s, and this is due to fibre failure observed only in the first 45° ply. The reduction of 7% in residual strength for centre impacted laminate at 150 m/s is due to fibre failure in the top 45°, 90° and -45° plies. The projectile was aimed to hit the target at 1.5 mm from the edge, and at the centre of the laminate's width. Some of

the high C.V values in Table 3 may be due to some variability in exactly where the laminates were impacted and possible projectile's rotations once it leaves the sabot.

Figure 9 shows the relationship between the residual tensile strength and delamination area for edge and centre impacted laminates. In the case of the latter, the residual strength decreases with increasing delamination area. In the previous section, it was shown that edge impacted laminates have a decreasing delamination area as impact velocity increases above 300 m/s. With increasing delamination up to 300 m/s followed by decreasing delamination area beyond 300 m/s, the residual strength of edge impacted laminates continues to decrease. This suggests that beyond 300 m/s, the reduction in residual tensile strength is mainly driven by the amount of fibre fracture and the effect of delamination area, if any, on the residual strength reduction is insignificant. The same cannot be said for centre impacts because the impact velocity after which delamination area might decrease has not been reached.

As the impact velocity is increased, impacted laminates showed increasing fibre fracture widths. The relationship between residual strength and fibre fracture width is depicted in Figure 10, where the residual tensile strength of impacted laminates decreases with increasing fibre fracture width. Although larger fibre fracture width and smaller delamination area are observed in edge impacted laminates at maximum impact velocity, the residual strength of edge impacted laminates is slightly higher than centre impacted laminates at maximum velocity. This implies that the very large delamination areas observed in centre impacted laminates may affect the residual strength. As such, it is important to characterise impact damage in terms of the extent of fibre failure and delamination area. In addition, since the presence of the large

damaged areas at several interfaces may contribute to strength reduction, it is best to represent the delamination area as an average of all interfaces showing delamination, instead of a maximum value.

3.3. Comparison with machined notches

The residual tensile strengths of unnotched, impacted and machined notch laminates are plotted against the fibre fracture widths, as shown in Figure 11 and Figure 12. From Figure 11, the edge-notch results are quite close to the edge impact results, except for the case of fibre fracture width equal to 1.33 mm. This is because the edge impacted laminate showed only one 0° ply broken, while the edge-notched laminate had all four 0° plies broken. The residual strength of the centre notches is quite close to the centre impacts for small fibre fracture widths, but as the fibre fracture width increases, the residual strengths of the centre impacted laminates fall further. This is believed to be due to the larger delamination areas that accompany the fibre fracture widths.

4. Discussion

For both edge and centre impacts, there was a significant amount of delamination and fibre fracture observed in most laminates for all varying impact velocities. In the present study, the ballistic limit is associated with the minimum impact velocity required for complete laminate perforation. Laminate perforation is observed at 300 m/s and 350 m/s for edge and centre impacts respectively. In an experimental study conducted by *Pernas-Sanchez et al.* [21] to investigate the effect of obliquity on carbon/epoxy laminate response, the damaged areas for normal and oblique impacts were observed to increase up to complete perforation of the

laminates. From that moment, the spherical projectile passes through the laminate and a smaller damaged area with increasing velocity was observed. A similar trend is observed in the edge impacted laminates, which show decreasing delamination area beyond 300 m/s. This is due to much more localised impact damage induced by the projectile beyond 300 m/s, resulting in the delamination area decreasing with increasing impact velocity. For centre impacts, further impacts tests at velocities higher than 350 m/s are required to see if the trend persists.

For edge impacted laminates having all 0° plies broken, edge machined notches of equivalent size give similar results, slightly overpredicting the residual tensile strength by an average difference of 5.4 %. With reasonably low percentage difference between the residual tensile strength of edge impacted and edge-notched laminates, it can be said that the residual strength of edge impacted laminates is mainly governed by the fibre fracture width. For small fibre fracture widths, centre impacted laminates have three broken 0° plies out of the four 0° plies and their residual strengths are quite close to those with centre machined notches of equivalent size, differing by an average of 7%. However, for large fibre fracture widths, centre machined notches are unconservative due to the large delamination areas in the impacted laminates. As such, the strength degradation in centre impacted laminates at high impact velocities is governed by the extent of fibre fracture and delamination area.

The damage zones in impacted and notched laminates are analysed to explain the discrepancies and similarities observed in their residual strengths for large fibre fracture widths. For machined notch laminates, interrupted tests that were stopped at 95% of the average failure load, P_{failure} , were carried out for specimens with an edge

notch length of 7.53 mm and a centre notch length of 6.95 mm. The specimens from the interrupted tests were then examined by CT scanning. The damage zone in the notched laminate was defined as the average distance between the crack tip and the last split in the 0° plies. For the impacted laminates, the impact induced damage zone can be quantified as the distance ahead of the impact damage front up to the furthest split in the 0° ply. Figure 13(a and b) show the comparison between the central 0° ply block in centre impacted and notched laminates. Prior to applied tensile loading, the centre impacted laminate shows a much larger damage zone (8.38 mm) compared to the damage zone (3.76 mm) observed in the centre-notched laminate at 95% of the failure load. Consequently, the lower residual tensile strength of the centre impacted laminates compared to the centre-notched laminates can be explained by the much larger damage zone. While Figure 13c illustrates the central 0° ply block in the edge impacted laminate before tensile loading, Figure 13d shows the central 0° ply block in an edge-notched laminate at 95% of the failure load. The damage zones measured in the edge impacted and edge-notched laminates are 2.21 mm and 2.32 mm respectively. Therefore, as the damage zone sizes are quite similar, an edge machined notch provides a reasonable equivalence in terms of residual tensile strength for this case.

5. Conclusion

The residual tensile strength of quasi-isotropic IM7/8552 thin composite laminates was investigated for high velocity oblique impacts at the edge and at the centre of the laminates. The fibre fracture width increases with impact velocity for both impact configurations. For edge impacted laminates, the delamination area

increases with impact velocity up to 300 m/s at which point the laminate is perforated, and it decreases in size with further increase in velocity. For centre impacted laminates, the delamination area increases with impact velocity, and complete perforation occurs at 350 m/s.

The residual tensile strength decreases as the fibre fracture width and delamination area vary with increasing impact velocity. At the maximum velocity, a centre impacted laminate revealed a 65% reduction in residual strength compared to a 60% reduction in residual strength for an edge impacted laminate. The residual strength of impacted laminates is strongly dependent on the extent of fibre fracture for all impact cases. The importance of delamination area to the strength degradation becomes increasingly relevant when it is large enough, as observed in centre impacted laminates at high velocities. Machined notches have been shown to provide a good representation of impacted laminates in terms of residual strength provided that all plies are broken and the damage zones around the impact point are small.

Acknowledgements

The authors acknowledge support from Rolls-Royce plc for this research through the Composites University Technology Centre (UTC) at the University of Bristol and from the Engineering and Physical Sciences Research Council (EPSRC) through the Centre for Doctoral Training in Advanced Composites at the University of Bristol (Grant no.EP/L016028/1). The authors also acknowledge the technical staff at the Department of Engineering Science at the University of Oxford for access to testing facilities and their support, as well as Dr Oliver Nixon-Pearson at the University of Bristol for carrying out the CT scanning of impacted laminates.

References

- [1] Abrate S. Impact on laminated composites. *Applied Mechanics Review* Jan 1991;44(4),155-190.
- [2] Ryan S, Schafer F, Guyot M, Hiermaier S, Lambert M. Characterising the transient response of CFRP/Al HC spacecraft structures induced by space debris impact at hypervelocity. *Int J Impact Eng* 2008;5:1756-63.
- [3] Cantwell WJ, Morton J. Comparison of the low and high velocity impact response of CFRP. *Comp* 1989;20:545-51.
- [4] López-Puente J, Zaera R, Navarro C. Experimental and numerical analysis of normal and oblique ballistic impacts on thin carbon/epoxy woven laminates. *Compos A* 2008;39:374-87.
- [5] Harper CA. *Handbook of plastics, elastomers, and composites*. 4th ed, New York: McGraw-Hill, 2002,236.
- [6] Cantwell WJ, Morton J. The impact resistance of composite materials – a review. *Compos* 1991;2:347-61.
- [7] Hou JP, Ruiz C. Soft body impact on laminated composite materials. *Compos A* 2007;38:505–15.
- [8] Kim H, Welch DA, Kedward KT. Experimental investigation of high velocity ice impacts on woven carbon/epoxy composites panels. *Compos A* 2003;34:25–41.
- [9] Hanada T, Liou JC. Comparison of fragments created by low- and hypervelocity impacts. *Adv Space Res* 2008;41:1132–7.
- [10] Hazell PJ, Kister G, Stennett C, Bourque P, Cooper G. Normal and oblique penetration of woven CFRP laminates by a high velocity steel sphere. *Compos A* 2008; 39:866–74.

- [11] Hazell PJ, Appleby-Thomas G. A study on the energy dissipation of several different CFRP-based targets completely penetrated by a high velocity projectile. *Comp Struct* 2009;91:103–9.
- [12] Hazell PJ, Appleby-Thomas G, Kister G. Impact, penetration, and perforation of a bonded carbon-fibre-reinforced plastic composite panel by a high-velocity steel sphere: an experimental study. *J Strain Analysis* 2010;45:439–50.
- [13] Ryan S, Schafer F, Riedel W. Numerical simulation of hypervelocity impact on CFRP/Al HC SP spacecraft structures causing penetration and fragment ejection. *Int J Impact Eng* 2006;33:703–12.
- [14] Cui H, Thomson D, Eskandari S, Petrinic N. A critical study on impact damage simulation of IM7/8552 composite laminate plate. *Int J Impact Eng* 2019;127:100-109.
- [15] Dorey G, Sidey GR. Residual strength of CFRP laminates after ballistic impact. In: *Proceedings of Mechanical properties high rates strain conference*. Oxford. 1974. p 344-351.
- [16] Wang J, Callinan R. Residual strengths of composite structures subjected to ballistic impact. *Comp Structures* 2014;117:423-432.
- [17] Romano F, Di Caprio F, Mercurio U. Compression after impact analysis of composite panels and equivalent hole method. *Procedia Eng* 2016;167:182-189.
- [18] Nettles AT. Notched compression strength of 18-ply laminates with various percentages of 0 plies. *Compos Mater* 2014;49(4):495-505.
- [19] Puhui C, Zhen S, Junyang W. A new method for compression after impact strength prediction of composite laminates. *Compost Mater* 2002;36:589-610.

- [20] Wallin M, Saarela O. Compression strength of notched and impact damaged composite laminates. In: Proceedings of 26th Congress of the International Council of the Aeronautical Sciences. Anchorage, Alaska, USA, 14th – 19th Sept 2008.
- [21] Pernas-Sanchez J, Artero-Guerrero JA, Varas D, Lopez-Puente J. Experimental analysis of normal and oblique high velocity impacts on carbon/epoxy tape laminates. *Compos A* 2014;60:24-31.
- [22] Duo P, Korsunsky AM, Nowell D. Residual stresses induced by foreign object damage on gas turbine blades: an experimental approach, In: Proceedings of 12th International Conference on Experimental Mechanics, Politecnico di Bari, Italy, 29th August-2nd Sept 2004.
- [23] Nowell D, Duo P, Stewart IF. Prediction of fatigue performance in gas turbine blades after foreign object damage. *Int J Fatigue* 2203;25:963-969.
- [24] Jacobsen G. Mechanical Performance Characterization of Stretch Broken Carbon Fiber Materials. In: Proceedings of SAMPE '09 Spring Symposium Conference Proceedings, 18th-21st May 2009.
- [25] Xu X, Wisnom MR, Mahadik Y, Hallett SR. An experimental investigation into size effects in quasi-isotropic carbon/epoxy laminates with sharp and blunt notches. *Comp Sci Tech* 2014;100:220-227.
- [26] Green BG, Wisnom MR, Hallett SR. An experimental investigation into the tensile strength scaling of notched composites. *Compos Part A* 2007;38(3):867-78.
- [27] Xu X, Wisnom MR, Chang K, Hallett SR. Unification of strength scaling between unidirectional, quasi-isotropic, and notched carbon/epoxy laminates. *Compos Part A* 2016;90:296-305.

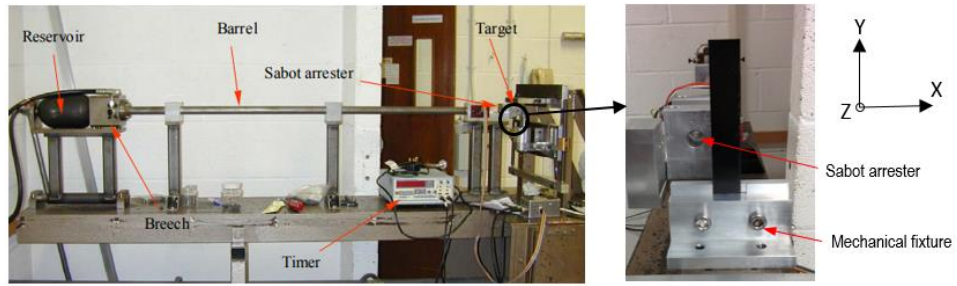


Figure 1: Gas gun facility used at the University of Oxford [23].

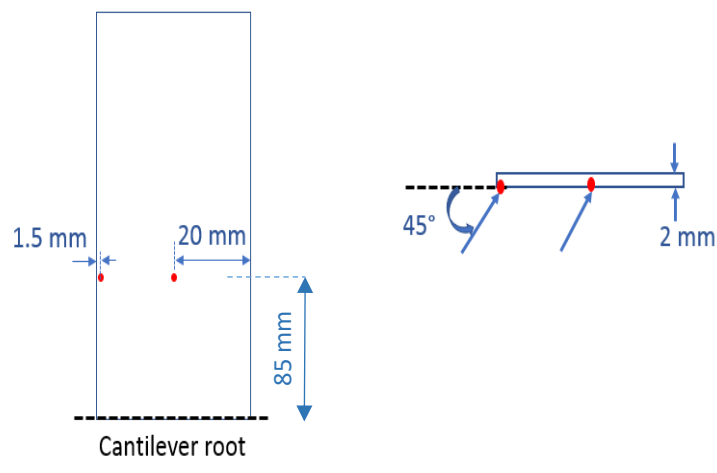


Figure 2: Impact positions shown in red on a laminate – front view (left), top view (right).

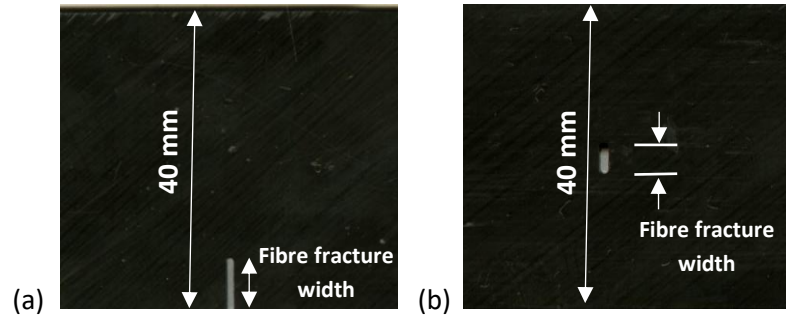


Figure 3: Typical (a) edge and (b) centre machined notches.

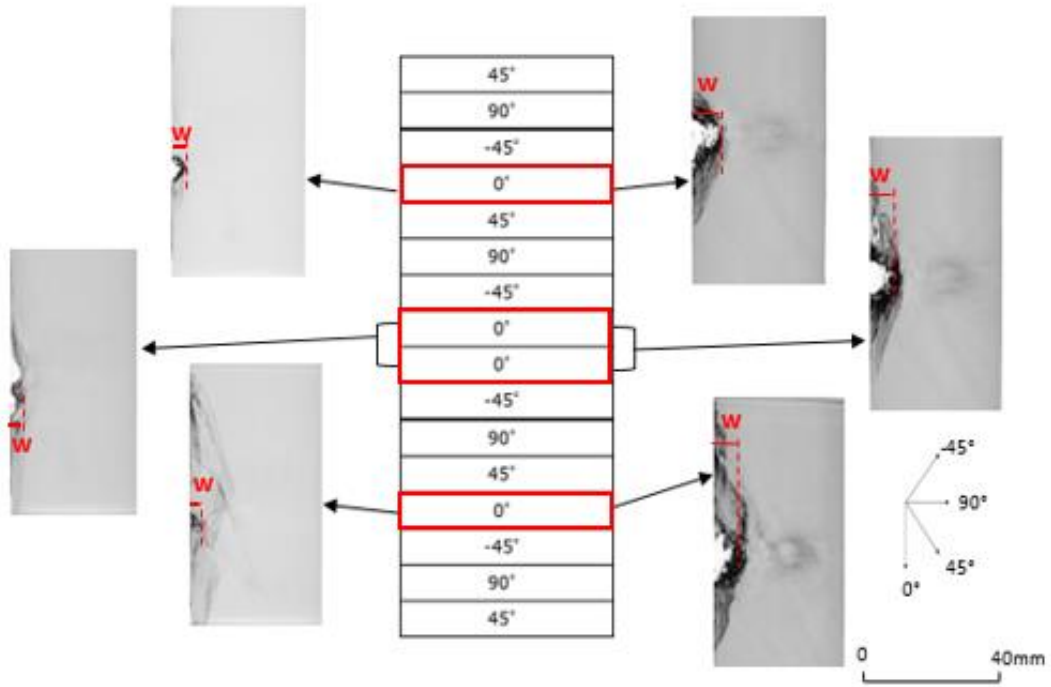


Figure 4: Fibre fracture width definition for edge impacted laminates at impact velocities 200 m/s (left) and 350 m/s (right).

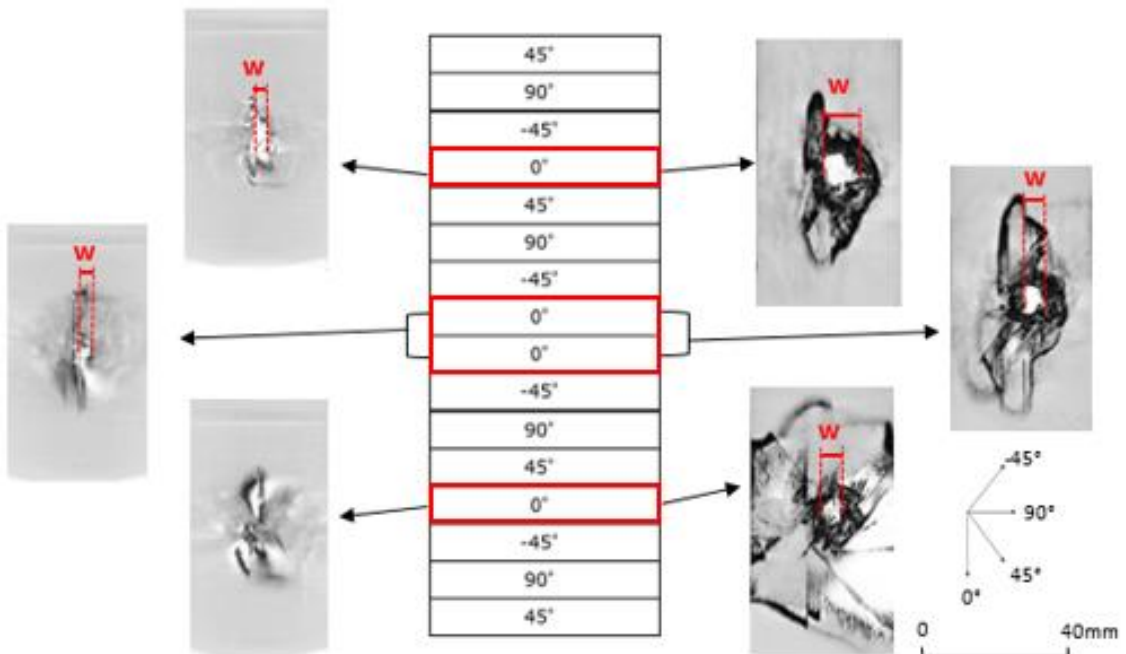


Figure 5: Fibre fracture width definition for centre impacted laminates at impact velocities 200 m/s (left) and 350 m/s (right).

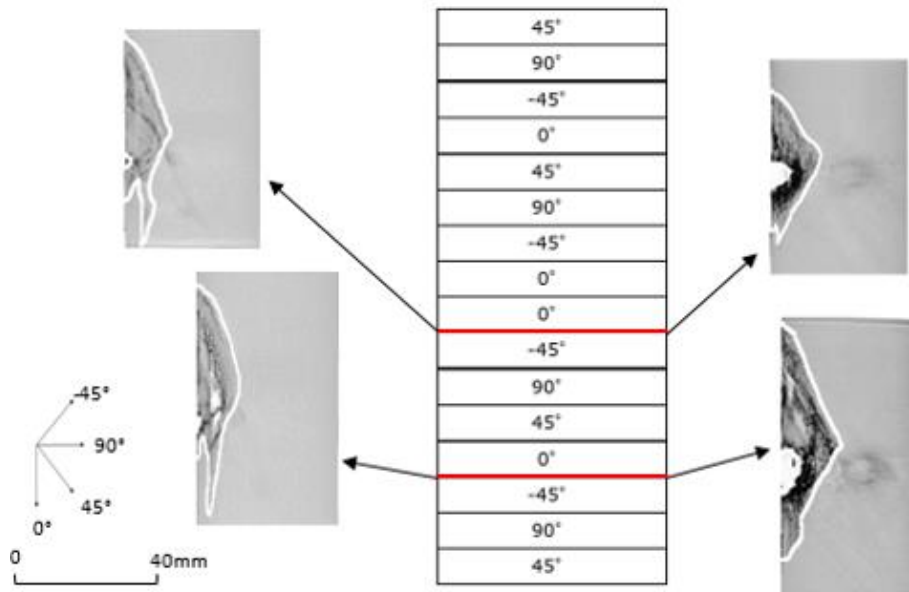


Figure 6: Delamination area at $-45^\circ/0^\circ$ interfaces represented within the white region for edge impacts at 200 m/s (left) and 350 m/s (right).

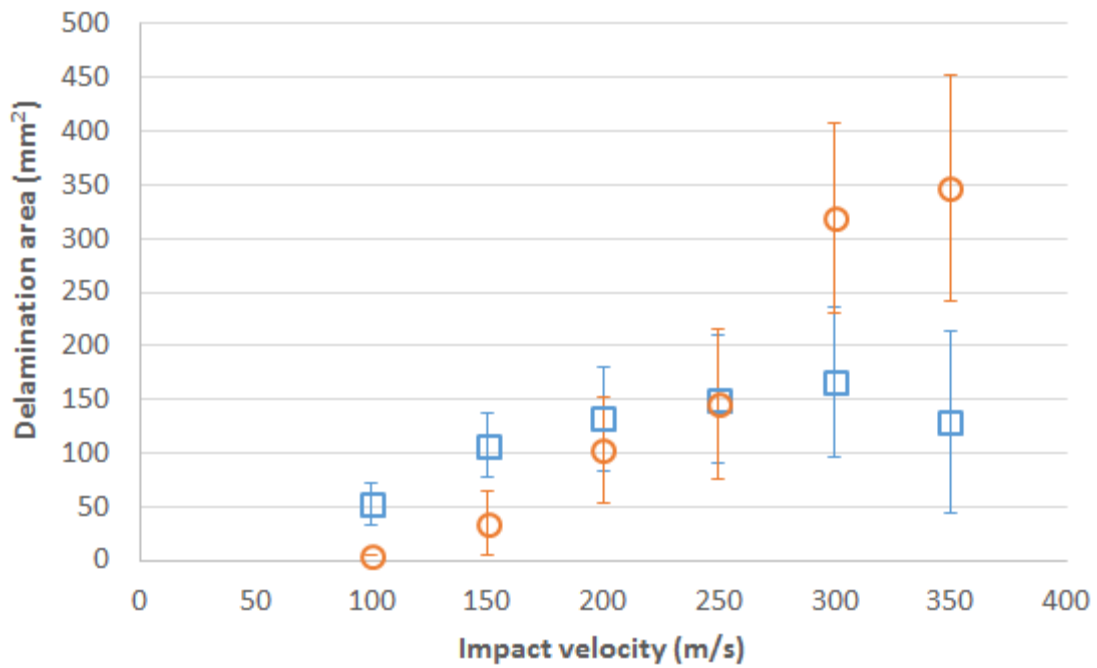


Figure 7: Delamination area versus impact velocity for edge and centre impacts.

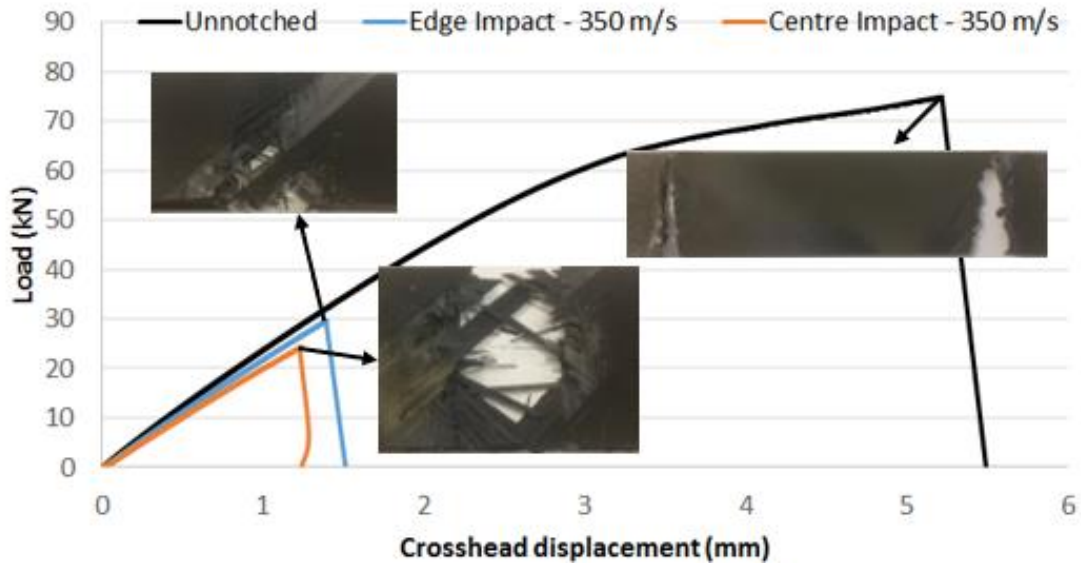


Figure 8: Typical load-displacement curve of the unnotched, edge and centre impacted laminates.

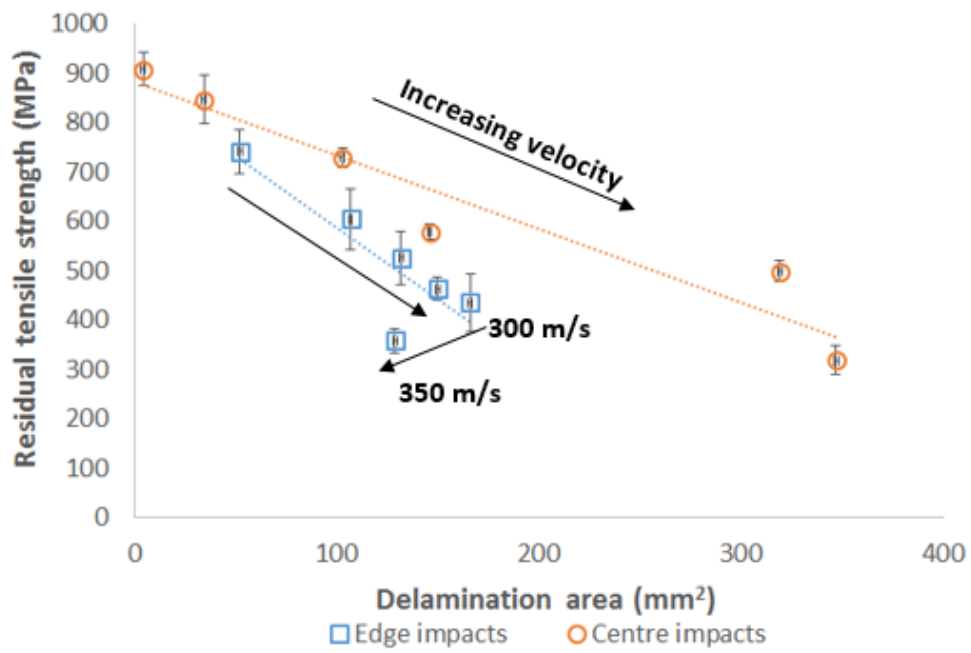


Figure 9: Residual tensile strength versus delamination area for edge and centre impacts.

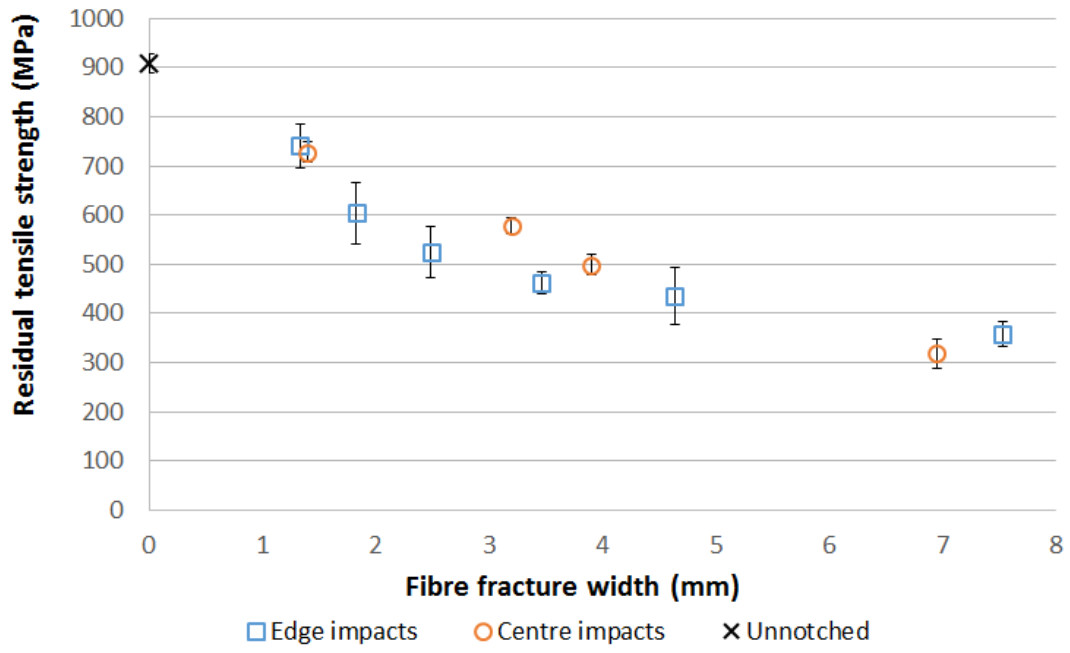


Figure 10: Residual tensile strength versus fibre fracture width.

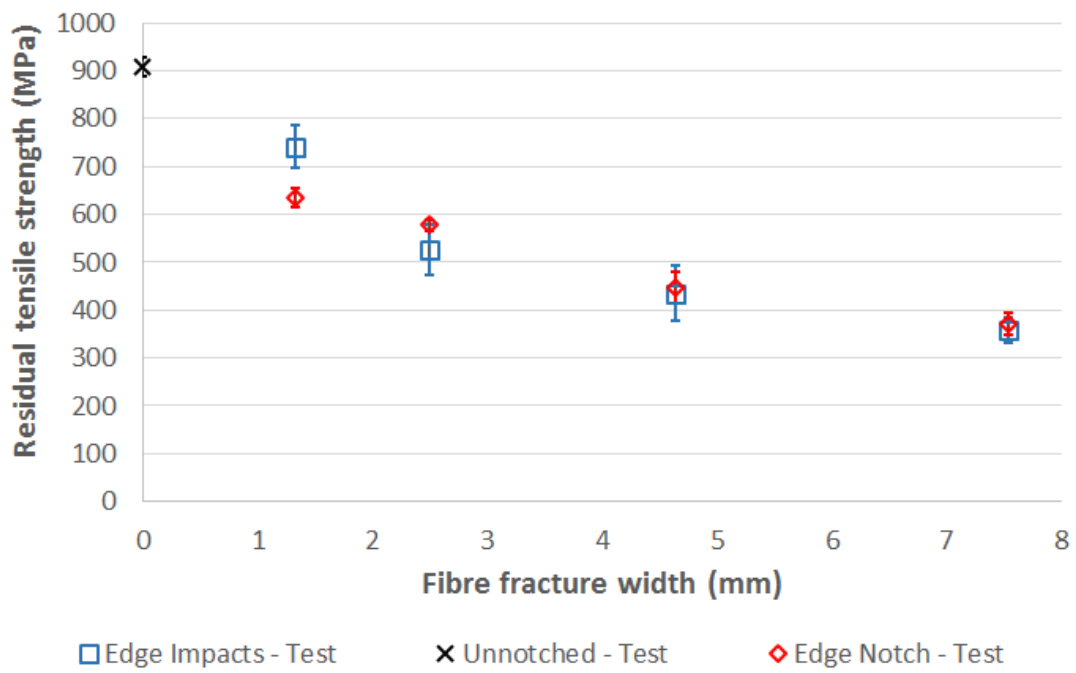


Figure 11: Residual tensile strength comparison between edge impacted and edge notched laminates.

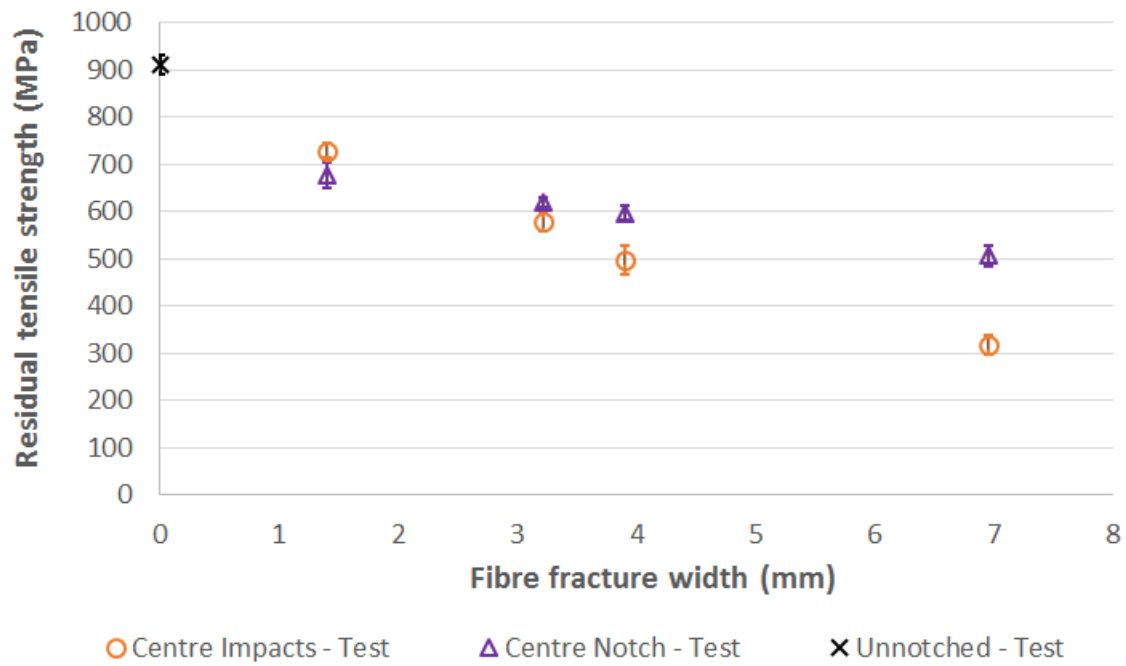


Figure 12: Residual tensile strength comparison between centre impacted and centre notched laminates.

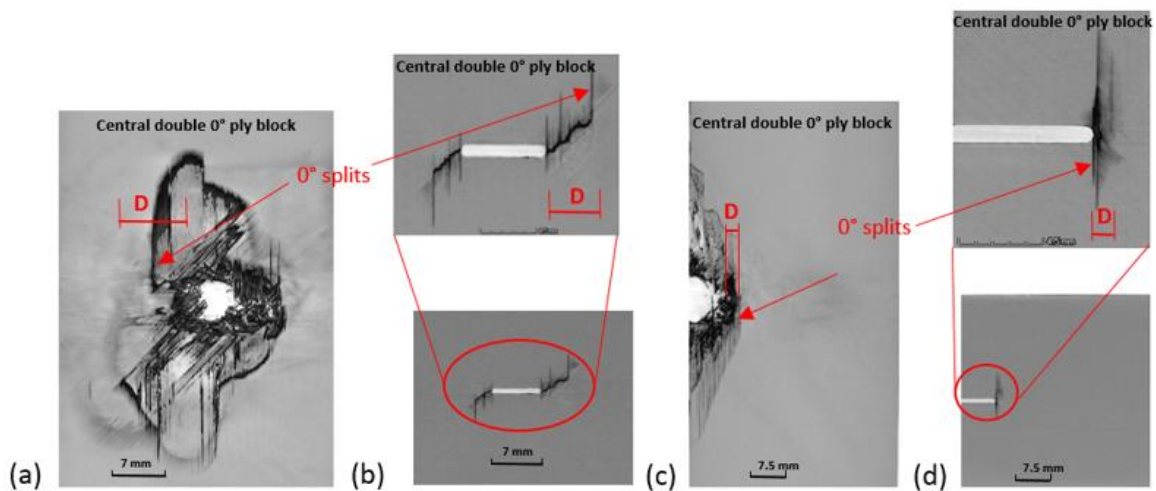


Figure 13: Central 0° ply block from (a) centre impacted laminate at 350 m/s, (b) centre-notched laminate (notch length = 6.95 mm), (c) edge impacted laminate at 350 m/s and (d) edge-notched laminate (notch length = 7.53mm). D is the damage zone size.

Table 1: Recorded impact velocities for each configuration.

| Edge Impacts | | Centre Impacts | |
|------------------|--|------------------|--|
| No. of specimens | Recorded impact velocity (m/s) (C.V %) | No. of specimens | Recorded impact velocity (m/s) (C.V %) |
| 4 | 98.0 (4.3) | 5 | 101 (5.4) |
| 4 | 150 (1.4) | 4 | 152 (1.1) |
| 4 | 201 (3.5) | 5 | 202 (0.7) |
| 4 | 256 (2.5) | 5 | 252 (0.5) |
| 5 | 308 (2.2) | 5 | 301 (1.2) |
| 4 | 351 (3.3) | 5 | 350 (1.2) |

Table 2: Fibre fracture width values for edge and centre impacts.

| Edge Impacts | | | Centre Impacts | |
|-----------------------|-----------------------|---------------------------|-----------------------|---------------------------|
| Impact velocity (m/s) | No of 0° plies broken | Fibre fracture width (mm) | No of 0° plies broken | Fibre fracture width (mm) |
| 100 | 1 | 1.33 | 0 | - |
| 150 | 1 | 1.83 | 0 | - |
| 200 | 4 | 2.49 | 3 | 1.40 |
| 250 | 4 | 3.46 | 3 | 3.22 |
| 300 | 4 | 4.64 | 3 | 3.90 |
| 350 | 4 | 7.53 | 4 | 6.95 |

Table 3: Tensile test results for impacted laminates.

| Impact velocity (m/s) | Residual tensile strength (MPa) (C.V.%) | | | |
|--|---|------------------|-----------|------------------|
| | Edge | No. of specimens | Centre | No. of specimens |
| 100 | 741 (6.0) | 3 | 908 (3.8) | 4 |
| 150 | 604 (15) | 3 | 846 (5.8) | 3 |
| 200 | 525 (12) | 3 | 728 (2.8) | 4 |
| 250 | 463 (4.0) | 3 | 578 (2.7) | 4 |
| 300 | 435 (13) | 4 | 498 (4.3) | 4 |
| 350 | 358 (7.1) | 3 | 318 (9.4) | 4 |
| Non-impacted laminate (5 specimens) = 909 MPa (2.2%) | | | | |